HAYATI
Journal of Biosciences

Vol. 33 No. 4, July 2026 1084-1099
DOI:10.4308/hjb.33.4.1084-1099
ISSN: 1978-3019
EISSN: 2086-4094

Research Article

Check for updates

OPEN ACCESS

The Complete Chloroplast Genome of *Melocanna baccifera* (Poaceae: Bambusoideae) and its Phylogenetic Implications

Thu-Thao Thi Huynh[1], Nga Thi Nguyen[1], Phi Anh Ngoc Nguyen[2], Anh-Duy Hoang Nguyen[3], Minh Trong Quang[3*]

[1]*Department of Hematology, Faculty of Medical Laboratory, Hong Bang International University, Ho Chi Minh City, Vietnam*
[2]*School of Medicine, Tan Tao University, Tay Ninh, Vietnam*
[3]*Department of Microbiology – Parasitology, School of Pharmacy, University of Medicine and Pharmacy at Ho Chi Minh City, Ho Chi Minh City, Vietnam*

ARTICLE INFO

Article history:
Received November 26, 2025
Received in revised form March 10, 2026
Accepted May 5, 2026
Available Online May 22, 2026

KEYWORDS:
Bambuseae,
Melocanna baccifera,
phylogenomics

ABSTRACT

Melocanna baccifera is a morphologically distinctive bamboo species in the subfamily Bambusoideae (Poaceae), recognized by a combination of diagnostic vegetative and reproductive characteristics, yet its chloroplast (cp) genomic features and phylogenetic position remain poorly understood. This study aimed to sequence, assemble, and annotate the complete cp genome of *M. baccifera* and to evaluate its phylogenetic implications within Bambusoideae. The complete cp genome of *M. baccifera* was *de novo* assembled into a 139,345 bp circular molecule with a typical quadripartite structure and a GC content of 38.9%. It comprised a large single-copy region of 82,927 bp, a small single-copy region of 12,768 bp, and a pair of inverted repeat regions of 21,825 bp each. The genome encoded a total of 129 genes, including 83 protein-coding genes, 38 transfer RNA genes, and eight ribosomal RNA genes. Comparative analysis showed that the cp genome of *M. baccifera* was similar to those of other Bambusoideae species in genome size, nucleotide composition, and gene content. Phylogenetic analysis placed *M. baccifera* in a well-supported clade with *Schizostachyum* species, consistent with currently recognized relationships within Bambusoideae. These findings provide a valuable plastid genomic resource for *M. baccifera* and improve our understanding of its evolutionary relationships, thereby offering a molecular foundation for future phylogenomic and evolutionary studies of bamboos.

1. Introduction

Melocanna baccifera (Roxb.) Kurz, locally known as "Tre lê" in Vietnam, is a bamboo species of ecological and socioeconomic significance in tropical Asia, distinguished by its monocarpic reproductive cycle and large fleshy fruits (Koshy *et al*. 2022). This species exhibits broad ecological adaptability and supports multiple human uses, including construction, food supply, livelihood support, and carbon sequestration (Rathour *et al*. 2022). Despite its ecological and socioeconomic importance, *M. baccifera* faces increasing pressure from habitat fragmentation and overexploitation, creating a need for genomic resources to inform conservation and management strategies (Wang *et al*. 2025). The taxonomic position of *M. baccifera* within the subfamily Bambusoideae has remained contentious due to morphological convergence and the lack of molecular data (Kelchner *et al*. 2013). In a previous study, the genus *Melocanna* has been placed within the tribe Bambuseae,

*Corresponding Author
E-mail Address: qtminh@ump.edu.vn

subtribe Melocanninae, based primarily on reproductive morphology and culm characteristics (Sutherland *et al*. 1987). However, recent molecular phylogenetic studies using plastid and nuclear markers have often produced incongruent topologies and weak statistical support for relationships among bamboo lineages, particularly within Paleotropical woody bamboos (Kelchner *et al*. 2013; Chalopin *et al*. 2021). This taxonomic uncertainty complicates efforts to interpret patterns of bamboo evolution and biogeography.

Chloroplast (cp) genomes have become a powerful tool for resolving complex phylogenetic relationships in plant systematics, offering numerous advantages over single-gene approaches (Wicke *et al*. 2011; Quang and Huynh 2024). Complete cp genomes provide extensive sequence data with variable evolutionary rates, enabling robust phylogenetic reconstruction across taxonomic levels (Parks *et al*. 2009; Le *et al*. 2025). Angiosperm cp genomes typically exhibit a quadripartite structure, consisting of large single-copy (LSC) and small single-copy (SSC) regions separated by a pair of inverted repeat regions (IRs), with generally conserved gene content and organization that facilitate comparative genomic analyses (Jansen *et al*. 2007; Huynh *et al*. 2024). Furthermore, the predominantly maternal inheritance and relatively slow evolutionary rate of cp genomes increase their value for phylogeographic and species-level phylogenetic investigations (Shaw *et al*. 2007). In recent years, the application of complete cp genomes in bamboo systematics has increased, and cp genome sequences are now available for several economically important species (Zhang *et al*. 2012; Ma *et al*. 2014). These studies have revealed structural variation among bamboo cp genomes, including gene loss, pseudogenization, and variation in intergenic spacer regions (Liu *et al*. 2020). However, cp genome sampling has remained strongly biased toward temperate bamboos, while tropical bamboo taxa, which harbored the highest species diversity, remain underrepresented (Wang *et al*. 2020).

Current phylogenetic hypotheses for bamboos have relied largely on analyses of a few plastid markers, such as *matK*, *rbcL*, and *ndhF*. Although these loci have provided important insights into bamboo evolution, they have often failed to resolve many relationships within the group (Sungkaew *et al*. 2009; Triplett and Clark 2010). The use of multigene datasets combining plastid and nuclear markers has improved phylogenetic resolution. Still, it has also revealed substantial incongruence between genomic compartments, pointing to complex evolutionary processes such as hybridization and incomplete lineage sorting (Fisher *et al*. 2014). In addition, surveys of published phylogenetic studies and available cp genome databases have shown that cp sequences remain limited for Bambuseae, despite the tribe's high species diversity and broad distribution across tropical Asia (Vorontsova *et al*. 2017; Wang *et al*. 2020). This shortage of genomic resources has constrained comprehensive phylogenetic reconstruction and comparative plastome analyses in bamboo.

The lack of a complete cp genome sequence for *M. baccifera* has limited detailed investigations of its plastome organization, gene content, and evolutionary relationships. Here, we aimed to sequence, assemble, and annotate the cp genome of *M. baccifera*, generating the plastid genomic resource for the genus *Melocanna*. Using these data, we characterized the main features of its cp genome and resolved the phylogenetic position of *M. baccifera* relative to the major bamboo lineages. Our study fills an important gap in bamboo genomics and provides a valuable resource for future research on phylogeny, evolution, and conservation.

2. Materials and Methods

2.1. Sample Collection and Processing

Fresh leaves of *M. baccifera* were collected from a mature individual plant in Tay Ninh Province, Vietnam (11°27′29.3″N, 106°21′01.8″E). Leaf tissues were immediately desiccated in silica gel at a tissue-to-desiccant ratio of 1:10. A voucher specimen was deposited at the School of Pharmacy, University of Medicine and Pharmacy at Ho Chi Minh City under voucher number UMP-TreLe-2024-01.

2.2. DNA Extraction and Assessment of Quality

Genomic DNA was extracted from leaf tissue using a modified CTAB protocol (Porebski *et al*. 1997). The extracted DNA was further purified using the Monarch Genomic DNA Purification Kit (T3010, New England Biolabs, USA). DNA quantity and purity were assessed on a NanoDrop One UV/Vis spectrophotometer (Thermo Fisher Scientific, USA). Samples with an A_{260}/A_{280} ratio of 1.8-2.0, A_{260}/A_{230} ratio of 2.0-2.2, and DNA concentrations ≥ 50 ng μL^{-1} were used for downstream analyses. Furthermore, DNA integrity was assessed by 1% agarose gel electrophoresis, confirming the presence of high-molecular-weight DNA without detectable degradation.

2.3. Genome Sequencing, Assembly, and Annotation

Library construction followed the manufacturer's protocol for the NEBNext Ultra II DNA Library Prep Kit for Illumina (E7103, New England Biolabs, USA), targeting an insert size of 350-450 bp. Whole-genome paired-end sequencing (2 × 150 bp) was performed on an Illumina MiSeq platform at KTest Science Co., Ltd. (Ho Chi Minh City, Vietnam). Raw reads were quality filtered using Trimmomatic v0.39 in paired-end mode (Phred+33, minimum read length 100 bp) (Bolger *et al*. 2014), yielding 9,553,764 paired-end reads of 150 bp. The cp genome was assembled using NOVOPlasty v4.3.5 (Dierckxsens *et al*. 2017) with both seed- and reference-assisted strategies, using *matK* (GenBank: EF125174) as the seed and *Schizostachyum auriculatum* (GenBank: NC_068071) as the reference. Gene annotation was performed with GeSeq with default settings (Tillich *et al*. 2017). Annotations of protein-coding genes were manually curated using BLAST (https://blast.ncbi.nlm.nih.gov/Blast.cgi) and by comparison with homologous sequences from related species, including *Schizostachyum dumetorum* (GenBank: LC590825) and *Schizostachyum diffusum* (GenBank: NC_063135). In addition, the annotation of tRNA genes was re-evaluated using tRNAscan-SE v2.0 (Chan *et al*. 2021). A circular cp genome map was generated using OGDRAW v1.3.1 (Greiner *et al*. 2019). The complete cp genome of *M. baccifera* was deposited in GenBank under accession number PX367280.

2.4. Comparative Genomic Analysis

For comparative plastome analyses, we retrieved complete cp genome sequences from representatives of the two major Bambuseae lineages, namely Paleotropical (*Bambusa utilis*, *Gigantochloa verticillata*, *Bonia saxatilis*, *Dendrocalamus bambusoides*, *Schizostachyum auriculatum*, and *Temochloa liliana*) and Neotropical woody bamboos (*Otatea glauca*, *Guadua angustifolia*, and *Chusquea culeou*). The junctions between the IRs and the single-copy regions (LSC and SSC), along with the adjacent genes, were examined using IRscope (Amiryousefi *et al*. 2018). Structural rearrangements involving *M. baccifera* and related plastomes were examined using MAUVE (Darling *et al*. 2004). Additionally, nucleotide diversity across the aligned plastomes was calculated in DnaSP v6 to identify highly divergent regions (Rozas *et al*. 2017).

2.5. Characterization of Long and Tandem Repeats and Analysis of Codon Usage Bias

Long repeats (including forward, reverse, palindromic, and complementary repeats) were identified using REPuter with the following criteria: ≥ 95% sequence identity, a Hamming distance of 3, and a minimum repeat length of 24 bp (Kurtz 2001). Tandem repeats were further detected with Phobos (via Geneious Prime) under default settings, applying minimum repeat-unit cutoffs of 10 for mononucleotide, 6 for dinucleotide motifs, 5 for tri- and tetranucleotide motifs, and 4 for penta- and hexanucleotide motifs (Telonis and Margarity 2015). Codon usage patterns and codon bias in the *M. baccifera* cp genome were evaluated using CodonW (https://github.com/lauringlab/CodonShuffle/tree/master/lib/codonW).

2.6. Phylogenetic Analysis

The phylogenetic reconstruction included 27 complete cp genomes representing Bambusoideae species and *Zizania palustris* from Ehrhartoideae as the outgroup (Table 1). Protein-coding sequences from the plastid genomes were extracted and aligned using MAFFT v7.487 (Katoh and Standley 2016). Gaps and poorly aligned regions were removed using trimAl v1.5.0 in the "automated1" mode (Capella-Gutiérrez *et al*. 2009). All retained CDS alignments were concatenated into a 111,211-site supermatrix using Geneious Prime v2025.0.2. Maximum-likelihood (ML) phylogenetic inference was conducted in IQ-TREE v2.1.3 (Minh *et al*. 2020). TVM+I was identified as the best-fitting nucleotide substitution model by ModelFinder (integrated in IQ-TREE) (Kalyaanamoorthy *et al*. 2017). Node support was assessed using 1,000 ultrafast bootstrap replicates. The resulting phylogenetic tree and associated bootstrap values were visualized using iTOL v7 (Letunic and Bork 2024).

3. Results

3.1. Chloroplast Genome Features of *Melocanna baccifera*

The complete cp genome of *M. baccifera* was a 139,345 bp circular molecule exhibiting the canonical quadripartite structure, comprising an LSC of 82,927 bp, an SSC of 12,768 bp, and two IRs of 21,825 bp each (Figure 1; Table 2). The overall GC content was 38.9%, with regional values of 36.9% in the LSC, 33.2% in the SSC, and 44.1% in the IRs. In total, the plastome

encoded 129 genes, including 83 protein-coding genes (PCGs), 38 transfer RNA (tRNAs), and eight ribosomal RNAs (rRNAs). A total of 19 genes were duplicated in the IR regions, including seven PCGs (*ndhB, rpl2, rps7, rps12, rpl23, rps19,* and *rps15*), eight tRNAs (*trnI-GAU, trnA-UGC, trnL-CAA, trnR-ACG, trnM-CAU, trnH-GUG, trnN-GUU,* and *trnV-GAC*), and all four rRNAs (*rrn4.5, rrn5, rrn16,* and *rrn23*). The trans-spliced *rps12* gene was identified, with its 5'exon located in the LSC and two 3' exons duplicated in the IR regions. Furthermore, 10 genes contained introns: nine PCGs (*atpF, ndhA, ndhB, petB, petD, rpl2, rpl16, rpoC1,* and *rps16*) harbored a single intron, whereas the *pafI* gene contained two introns.

3.2. The Chloroplast Genome Structures and Comparative Analyses among Bambuseae Species

Comparative analysis of plastome features revealed clear differences between the Paleotropical and Neotropical woody bamboo lineages within Bambuseae (Table 3). The sampled Paleotropical taxa, including *M. baccifera*, showed highly conserved plastome characteristics, with identical GC content values (38.9%) and a narrow range of total genome sizes (139,007-139,523 bp). Their regional lengths were also relatively uniform, with LSC regions ranging from 82,546 to 83,074 bp, SSC regions from 12,741 to 12,978 bp, and IR regions from 21,776 to 21,825 bp. In contrast, the sampled Neotropical taxa showed slightly lower GC content (38.7-38.8%) and generally smaller plastomes (135,331-138,137 bp). This difference was associated mainly with reduced IR lengths in *O. glauca* (20,333 bp) and *G. angustifolia* (19,797 bp), and with a shorter LSC region in *C. culeou* (81,672 bp). The plastome of *M. baccifera* (139,345 bp; 38.9% GC) fell within the conserved range observed for the Paleotropical lineage.

The MAUVE whole-plastome alignment showed that the eight Bambuseae cp genomes were highly conserved in overall structure (Figure 2). Most homologous regions formed shared locally collinear blocks (LCBs) arranged in the same order across taxa, indicating strong synteny and the absence of large-scale translocations or major inversions. The cp genome of *M. baccifera* exhibited an

Table 1. The taxa sampled and GenBank accession numbers used in the phylogenetic analyses

Species	GenBank accession	Tribe
Gigantochloa verticillata	MN688203	
Neomicrocalamus yunnanensis	NC_050767	
Dendrocalamus bambusoides	NC_050762	
Bambusa utilis	NC_063148	
Temochloa liliana	NC_085342	
Bonia saxatilis	NC_050756	
Schizostachyum dumetorum	LC590825	Bambuseae
Schizostachyum diffusum	NC_063135	
Schizostachyum auriculatum	NC_068071	
Melocanna baccifera	PX367280	
Otatea glauca	NC_028631	
Guadua angustifolia	NC_029749	
Chusquea culeou	NC_042672	
Cryptochloa strictiflora	JX235348	
Froesiochloa boutelouoides	NC_039983	Olyreae
Rehia nervata	NC_039984	
Pariana campestris	NC_027491	
Fargesia qinlingensis	MH988720	
Fargesia denudata	MH988724	
Arundinaria fargesii	MH988716	
Ampelocalamus scandens	MK393371	
Ampelocalamus gongshanensis	MK393373	
Drepanostachyum falcatum	MF460981	Arundinarieae
Chimonobambusa tumidinoda	MF066244	
Chimonobambusa sichuanensis	NC_056904	
Acidosasa purpurea	NC_015820	
Arundinaria appalachiana	NC_023934	
Zizania palustris	NC_066144	Outgroup

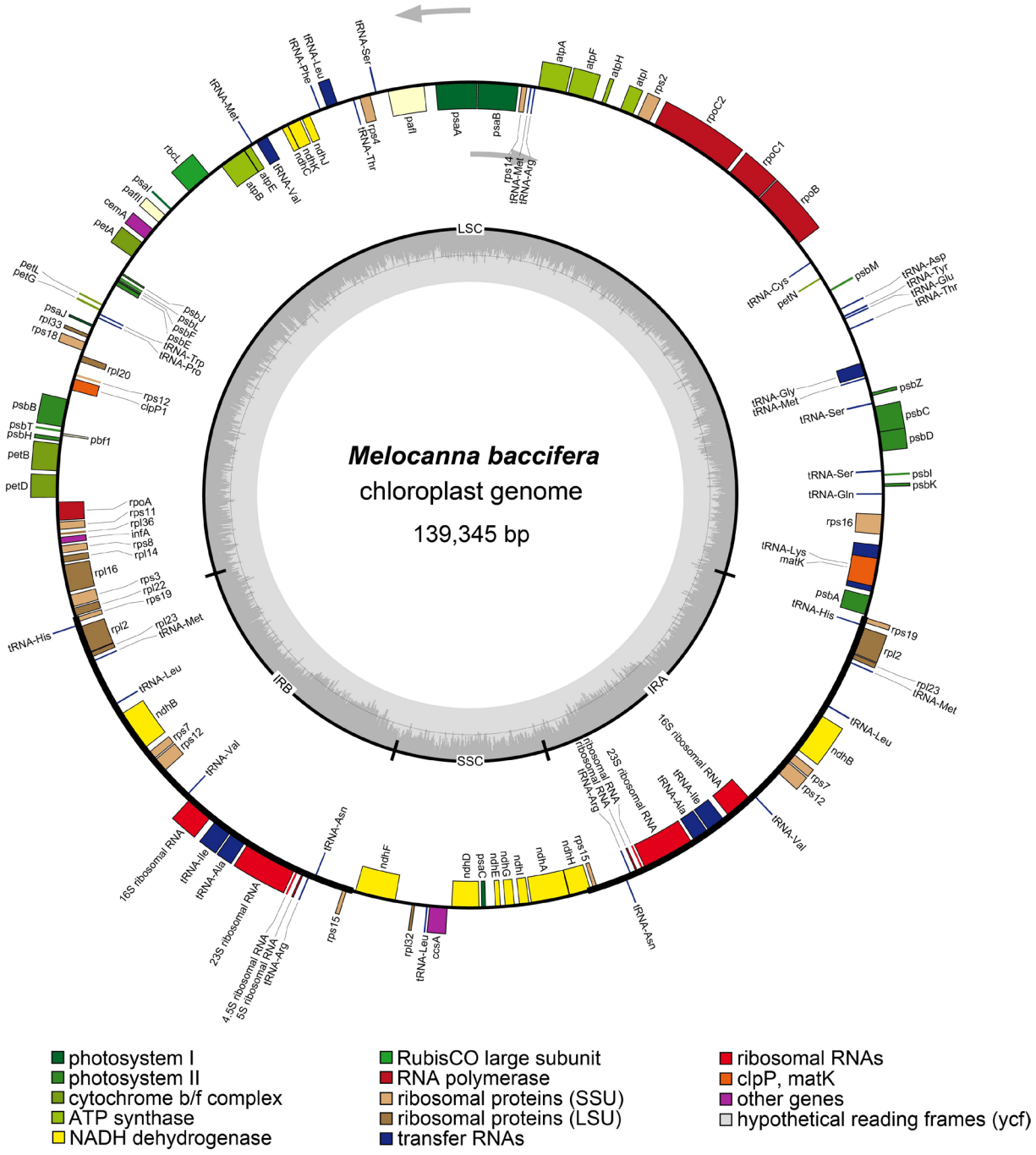

Figure 1. Circular map of the chloroplast genome of *Melocanna baccifera* (139,345 bp). The genome exhibits a typical quadripartite architecture comprising a large single-copy (LSC), a small single-copy (SSC), and two inverted repeat regions (IRa and IRb). Genes drawn outside the outer circle are transcribed clockwise, whereas those inside are transcribed counterclockwise. Gene functions are color-coded as indicated below the genome. The inner histogram depicts the GC content across the genome (the lighter background indicates the AT content)

Table 2. Gene content of the plastome of *Melocanna baccifera*

Category	Group of genes	Name of the genes
Genes involved in photosynthesis	Subunits of the ATP synthase	*atpA*[a], *atpB*, *atpE*, *atpF*, *atpH*, *atpI*
	NADH-dehydrogenase subunits	*ndhA*[a], *ndhB*[a] (2×), *ndhC*, *ndhD*, *ndhE*, *ndhF*, *ndhG*, *ndhH*, *ndhI*, *ndhJ*, *ndhK*
	Subunits of the cytochrome b/f complex	*petA*, *petB*[a], *petD*[a], *petG*, *petL*, *petN*
	Subunits of photosystem I	*psaA*, *psaB*, *psaC*, *psaI*, *psaJ*, *pafI*[b], *pafII*,
	Subunits of photosystem II	*psbA*, *psbB*, *psbC*, *psbD*, *psbE*, *psbF*, *psbH*, *psbI*, *psbJ*, *psbK*, *psbL*, *psbM*, *psbT*, *psbZ*, *pbf1*
	Rubisco subunit	*rbcL*
Self-replication	Large ribosome subunit	*rpl2*[a] (2×), *rpl14*, *rpl16*[a], *rpl20*, *rpl22*, *rpl23* (2×), *rpl32*, *rpl33*, *rpl36*
	Small ribosome subunit	*rps2*, *rps3*, *rps4*, *rps7* (2×), *rps8*, *rps11*, *rps12* (2×), *rps14*, *rps15* (2×), *rps16*[a], *rps18*, *rps19* (2×)
	DNA-dependent ribonucleic acid polymerase	*rpoA*, *rpoB*, *rpoC1*[a], *rpoC2*
	Transfer of RNA genes	*trnA-UGC*[a] (2×), *trnC-GCA*, *trnD-GUC*, *trnE-UUC*, *trnF-GAA*, *trnG-UCC*[a], *trnG-GCC*, *trnH-GUG* (2×), *trnI-GAU*[a] (2×), *trnK-UUU*[a], *trnL-CAA* (2×), *trnL-UAA*[a], *trnL-UAG*, *trnfM-CAU*, *trnM-CAU* (2×), *trnM-CAU*, *trnN-GUU* (2×), *trnP-UGG*, *trnQ-UUG*, *trnR-ACG* (2×), *trnR-UCU*, *trnS-GCU*, *trnS-GGA*, *trnS-UGA*, *trnT-GGU*, *trnT-UGU*, *trnV-GAC* (2×), *trnV-UAC*[a], *trnW-CCA*, *trnY-GUA*
	Ribosomal RNA	*rrn4.5* (2×), *rrn5* (2×), *rrn16* (2×), *rrn23* (2×)
Other genes	C-type cytochrome synthesis gene	*ccsA*
	Enveloped membrane protein	*cemA*
	Protease	*clpP1*
	The translational initiation factor	*infA*
	Maturase	*matK*

(2×) duplicated genes in IR regions, [a]genes harboring a single intron, [b]genes harboring two introns

Table 3. Chloroplast genome features of *Melocanna baccifera* and related Bambuseae species: GC content and region lengths

Organism	GenBank Accession no.	%GC	Length (bp)			
			Total	LSC	SSC	IRs
Melocanna baccifera[a]	PX367280	38.9	139,345	82,927	12,768	21,825
Gigantochloa verticillata[a]	MN688203	38.9	139,489	83,061	12,876	21,776
Bonia saxatilis[a]	NC_050756	38.9	139,007	82,546	12,839	21,811
Dendrocalamus bambusoides[a]	NC_050762	38.9	139,523	83,074	12,871	21,790
Bambusa utilis[a]	NC_063148	38.9	139,491	82,990	12,905	21,798
Schizostachyum auriculatum[a]	NC_068071	38.9	139,241	82,932	12,741	21,784
Temochloa liliana[a]	NC_085342	38.9	139,510	82,932	12,978	21,800
Otatea glauca[b]	NC_028631	38.8	136,377	82,841	12,870	20,333
Guadua angustifolia[b]	NC_029749	38.7	135,331	82,840	12,898	19,797
Chusquea culeou[b]	NC_042672	38.8	138,137	81,672	12,858	21,804

[a]Species belonging to the Paleotropical lineage; [b]Species belonging to the Neotropical lineage; LSC: large single-copy; SSC: small single-copy; IRs: inverted repeat regions

LCB pattern similar to those of the other sampled taxa, supporting a generally conserved plastome organization within Bambuseae.

The plastome length, regional composition, and IR junction architecture indicated that the cp genome of *M. baccifera* was structurally typical of bamboos and most similar to those of *Schizostachyum* species. Comparative analyses of IR boundaries further showed that the positions of the four junctions (JLB, JSB, JSA, and JLA) were largely conserved among the eight cp genomes (Figure 3). At the JLB (LSC/IRb) junction, *rpl22* was located in the LSC close to the junction (20-42

bp from junction), whereas *rps19* was positioned within the IRb near the junction (28-49 bp from junction). *ndhF* was consistently located in the SSC at the JSB (IRb/SSC) junction, beginning 101-114 bp from the junction. The JSA (SSC/IRa) junction was located within *ndhH* in all taxa. However, the gene length was constant (1,182 bp), its partitioning varied, with 933-1,069 bp in the SSC and 113-249 bp in IRa, reflecting minor expansion and contraction at this boundary. Finally, *psbA* was located in the LSC near the JLA (IRa/LSC) junction, occurring 0-113 bp from the boundary, with *T. liliana* showing the closest placement.

3.3. Repeat Structure and SSR Analyses

A total of 44 SSRs were identified in the *M. baccifera* cp genome. Mononucleotide repeats were the most abundant type (36; 81.8%), whereas di- and trinucleotide repeats were much less frequent (3 each; 6.8%), and only one tetranucleotide and one hexanucleotide repeat were detected (2.3% each), as shown in Figure 4. Most SSRs were located in the LSC region (36 repeats). In contrast, the SSC and IR regions together contained only 4 repeats in each. Among the mononucleotide motifs, poly-A repeats (n = 19) were slightly more common than poly-T repeats (n = 17). Among the remaining motif types, AT was the most frequent dinucleotide repeat (3 repeats), whereas GTT, TAG, AAG, CTTT, and ATCAAA each occurred only once. Overall, the SSR profile indicated a strong bias toward A/T mononucleotide repeats and an uneven distribution concentrated in the LSC region.

A total of 10 long repeats, including nine forward repeats and one palindromic repeat, were detected in the cp genome of *M. baccifera* (Table 4). The repeat lengths ranged from 26 to 104 bp, with most repeats falling between 30 and 61 bp. Long repeats were unevenly distributed across the plastome, with the majority located in the LSC region (7 repeats). In contrast, only two repeats, including the single palindromic repeat, were found in

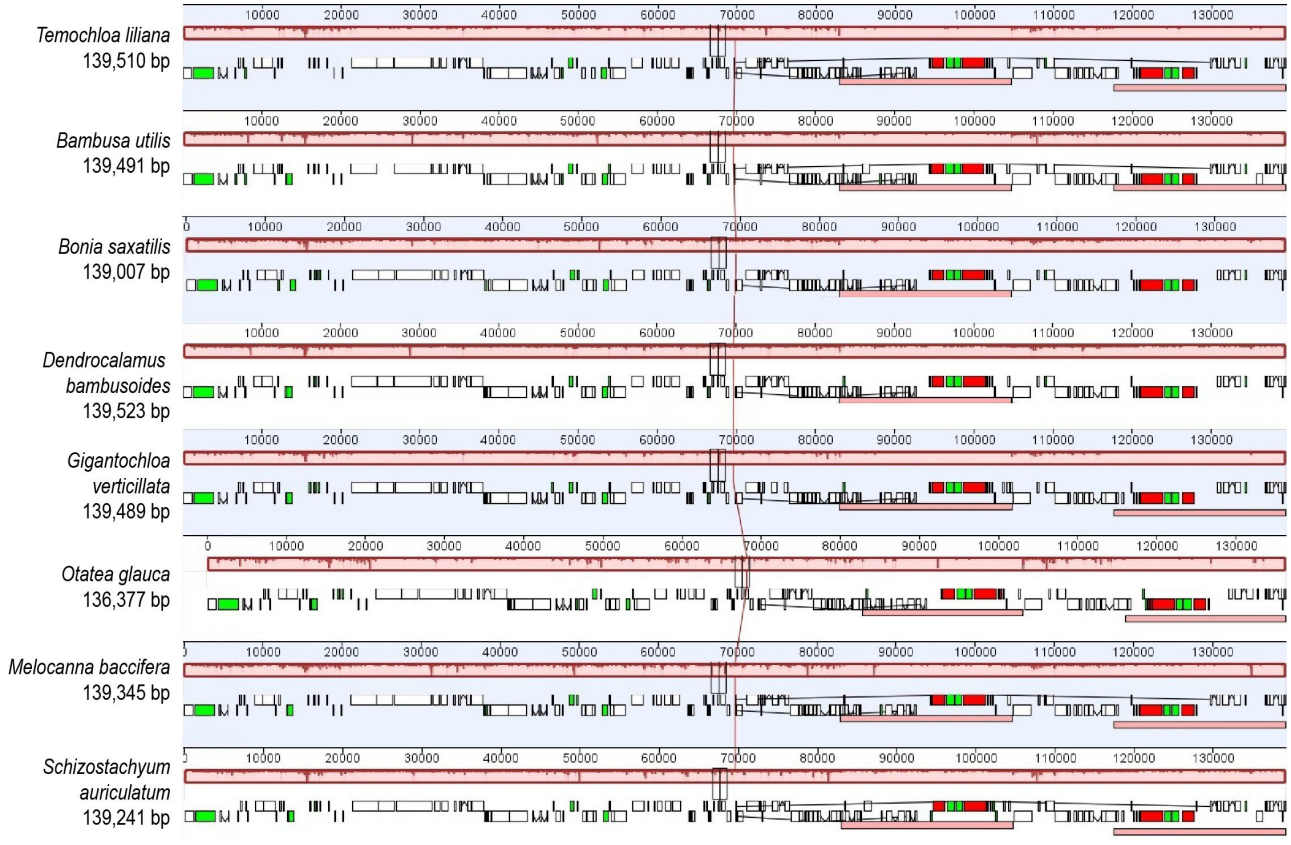

Figure 2. MAUVE alignment of eight Bambusoideae chloroplast genomes illustrating their structural conservation. Each horizontal track represents a chloroplast genome, with the species name and genome size shown on the left. Genome coordinates are indicated by the scale bar at the top. Colored blocks denote locally collinear blocks, which are homologous regions shared among the genomes. Connecting lines indicate the corresponding positions of these blocks across genomes. The red similarity profile above each genome indicates the relative sequence conservation across the alignment

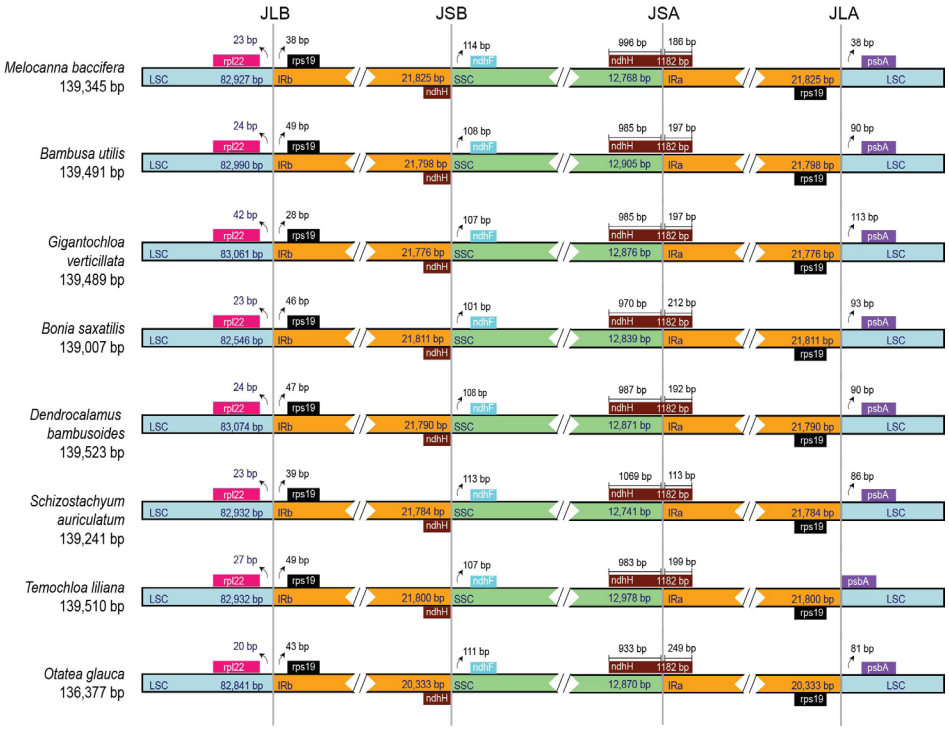

Figure 3. Comparison of chloroplast IR-SC boundary regions between *Melocanna baccifera* and related Bambuseae species. Boundaries are shown at four junctions: JLB (LSC/IRb), JSB (IRb/SSC), JSA (SSC/IRa), and JLA (IRa/LSC). The colored blocks represent genes adjacent to the junctions for each taxon, and the arrows indicate transcriptional orientation. The numbers above the blocks denote the distances (bp) from the gene ends to the junctions; values overlapping the junctions indicate partial gene copies (pseudogene fragments) within the IRs. The region lengths (LSC, SSC, and IR) are shown beneath each panel

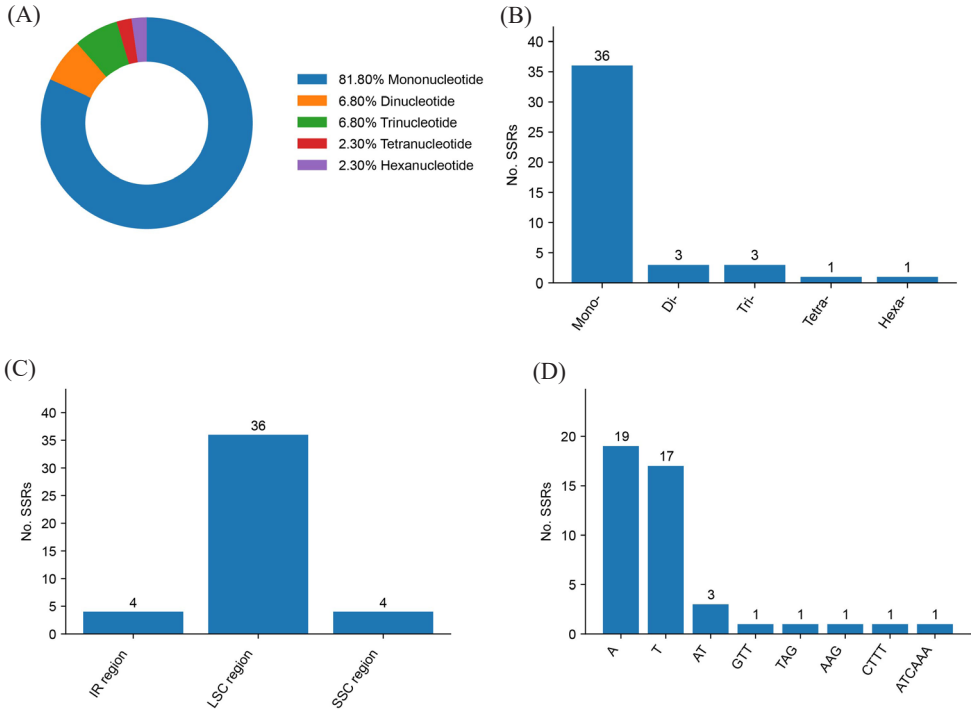

Figure 4. Distribution and characteristics of simple sequence repeats (SSRs) in the chloroplast genome of *Melocanna baccifera*. (A) Proportional composition of SSR motif types, showing the relative frequencies of mono-, di-, tri-, tetra-, and hexanucleotide repeats. (B) Number of SSRs for each repeat class. (C) Distribution of SSRs across chloroplast genome regions (LSC, SSC, and IR). (D) Frequency of detected SSR motifs, with counts labeled above each bar

the IR region. One forward repeat was positioned across the LSC/IR boundary. The longest repeat (104 bp) in the LSC was a forward repeat, highlighting this region as the main hotspot for long-repeat accumulation.

3.4. Sequence Divergence Analysis

Sliding-window analysis of Bambuseae cp genomes showed that nucleotide diversity (Pi) was low across most of the genomes, with only minor variation throughout (Figure 5). The strongest variation occurred in the LSC region, with the highest peak located in the *trnG-trnT* intergenic spacer. Apart from this hotspot, the LSC region remained relatively conserved. The IR regions (IRb and IRa) were the most conserved, with consistently low Pi values. The SSC region showed slightly higher and more uneven Pi values, with a few minor peaks of variation.

3.5. Codon Usage Bias Analysis

A total of 19,879 codons from the protein-coding sequences of the *M. baccifera* cp genome were counted (Table 5). Codon usage varied among amino acids: leucine was the most abundant (2,128 codons; 10.70%), followed by isoleucine (1,622; 8.16%), glycine (1,468; 7.38%), and serine (1,423; 7.16%). Cysteine was the least represented amino acid (217; 1.09%). RSCU analysis showed a clear codon usage bias, with preferred synonymous codon

Table 4. Long-repeat distribution and characteristics in the chloroplast genome of *Melocanna baccifera*

Type	Location	Length	Sequence
Palindromic	IR	26	ATTCTTTTATTTTAGATAGAAGAAAC
Forward	LSC	32	GAGGAAGACTCAGAAGACGAATATGGGAGCCC
Forward	LSC	35	ACCCTAGAAGACGAATATAGGACTCGAGAGGAAGA
Forward	LSC/IR	41	AATGTATGCATTTCGATTAGGGTCGTATTCTATGGTTACGA
Forward	LSC	44	CCCTCTACCATATCTATACAAATAGAATAGTCCATTTATACAGA
Forward	IR	49	TATCATATTCTATATATATAGAAATATCATAGAATAGACATATAGAATT
Forward	LSC	53	TTTTTTTCTCTCCTATTTTTTTTTTCTGTCATATTTTTTTCTCTCCTATTTTT
Forward	LSC	54	GTGGTAGAGTAATGCCATGGTAAGGCATAAGTCATCGGTTCAAATCC-GATAAAG
Forward	LSC	61	GAGGAAGACTCAGAAGACGAATATGGGAGCCCGGAGGAAGACT-CAGAAGACGAATATGGGA
Forward	LSC	104	ACCCTAGAGGACGAATATAGGACTCGAGAGGAAGACTCAGAGGAC-GAATATAGGAGCCCAGAGAACGGATATAGGACCCGAGAGGAC-GAATATGAAACCCTAGA

LSC: large single-copy; SSC: small single-copy; IR: inverted repeat region

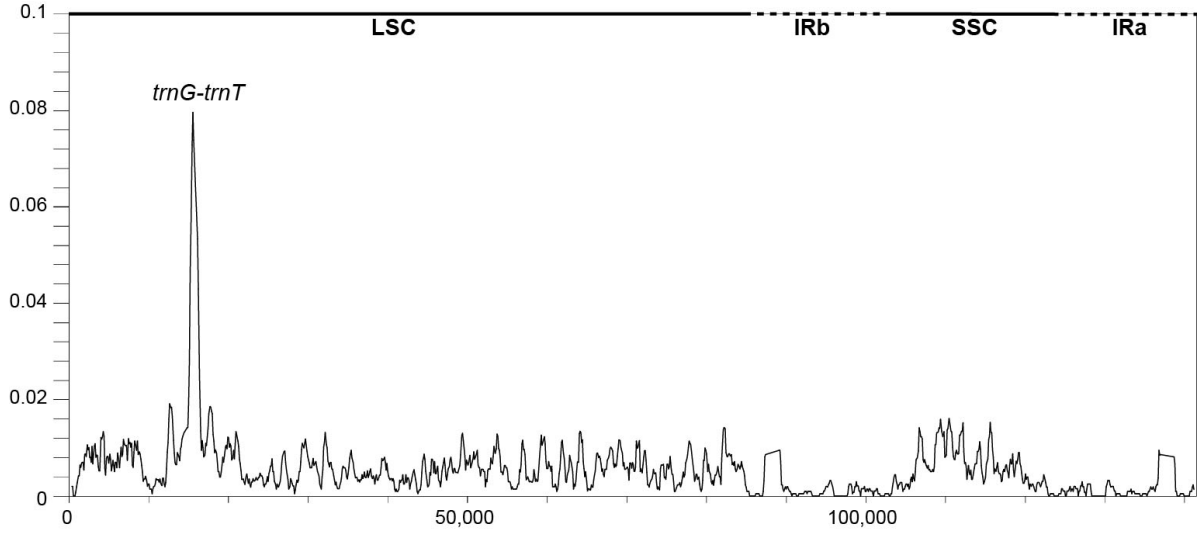

Figure 5. Sliding-window analysis of nucleotide diversity across the Bambuseae chloroplast genome. The x-axis indicates the genomic position, and the y-axis indicates the Pi values. The boundaries between the large single-copy (LSC), inverted repeat B (IRb), small single-copy (SSC), and inverted repeat A (IRa) regions are shown at the top. The highest diversity peak was located in the trnG–trnT intergenic region, indicating a potential hypervariable hotspot

Table 5. Relative synonymous codon usage (RSCU) values estimated from the chloroplast genome of *Melocanna baccifera*

Codon	AA	Freq	RSCU
GCA	A	372	1.18
GCC		190	0.60
GCG		151	0.48
GCT		546	1.74
TGC	C	49	0.45
TGT		168	1.55
GAC	D	163	0.45
GAT		555	1.55
GAA	E	777	1.49
GAG		265	0.51
TTC	F	393	0.72
TTT		706	1.28
GGA	G	580	1.58
GGC		150	0.41
GGG		274	0.75
GGT		464	1.26
CAC	H	118	0.52
CAT		333	1.48
ATA	I	496	0.92
ATC		320	0.59
ATT		806	1.49
AAA	K	730	1.43
AAG		291	0.57
CTA	L	320	0.9
CTC		148	0.42
CTG		115	0.32
CTT		453	1.28
TTA		699	1.97
TTG		393	1.11
ATA	M	1	0.01
ATG		465	2.98
GTG		2	0.01
AAC	N	200	0.51
AAT		583	1.49
CCA	P	231	1.07
CCC		202	0.94
CCG		102	0.47
CCT		328	1.52
CAA	Q	518	1.54
CAG		155	0.46
AGA	R	366	1.76
AGG		128	0.62
CGA		265	1.28
CGC		107	0.52
CGG		86	0.41
CGT		294	1.42
AGC	S	103	0.43
AGT		300	1.26
TCA		239	1.01
TCC		274	1.16
TCG		129	0.54
TCT		378	1.59
ACA	T	295	1.1
ACC		198	0.74
ACG		130	0.49
ACT		447	1.67
GTA	V	443	1.51
GTC		142	0.48
GTG		161	0.55
GTT		430	1.46
TGG	W	345	1
TAC	Y	152	0.42
TAT		572	1.58
TAA	*	45	1.63
TAG		21	0.76
TGA		17	0.61
Total		19,879 codons	

AA: amino acid; Freq: frequency of codon in chloroplast genome; RSCU: Relative Synonymous Codon Usage; *: stop codon

(RSCU > 1) predominantly ending in A or T at the third codon position (Figure 6). Overall, 32 codons had RSCU values greater than 1, and 29 of these ended in A/T, indicating a strong A/T preference in synonymous codon usage. Several amino acids displayed pronounced preferences for specific A/T-ending codons, such as GCT for alanine (RSCU = 1.74), GAT for aspartic acid (RSCU = 1.55), GAA for glutamic acid (RSCU = 1.49), TTT for phenylalanine (RSCU = 1.28), and TAT for tyrosine (RSCU = 1.58). Leucine showed strong codon bias, with TTA being the most favored codon (RSCU = 1.97), whereas CTG was markedly underrepresented (RSCU = 0.32). Among stop codons, TAA was the most frequently used (45 occurrences; RSCU = 1.63), followed by TAG (21; 0.76) and TGA (17; 0.61).

3.6. Phylogenetic Analysis

The ML analysis of the concatenated plastid protein-coding sequences recovered a well-resolved topology for Bambusoideae (Figure 7). Overall, the backbone received strong support, with 95% of internal nodes showing ultrafast bootstrap values ≥ 70%. The sampled taxa were clearly separated into three monophyletic tribes, Bambuseae, Olyreae, and Arundinarieae, all with strong support (bootstrap = 100). Two major lineages were recovered within Bambuseae, corresponding to the Paleotropical and Neotropical assemblages. The Paleotropical lineage included *Gigantochloa*, *Neomicrocalamus*, *Dendrocalamus*, *Bambusa*, *Temochloa*, *Bonia*, *Schizostachyum*, and *Melocanna*, whereas the

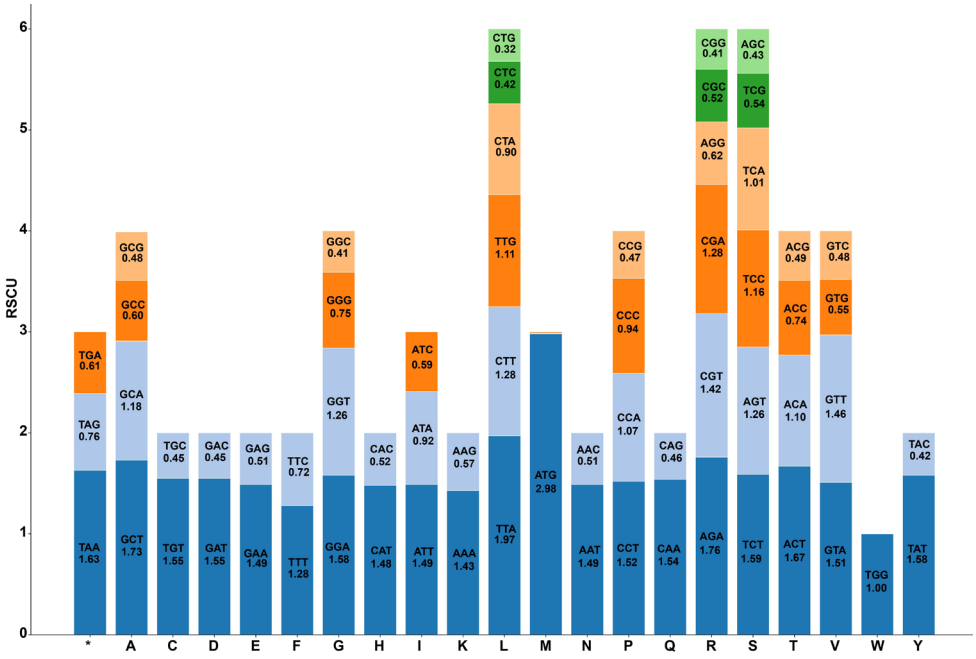

Figure 6. Relative synonymous codon usage (RSCU) in the chloroplast genome of *Melocanna baccifera*. Stacked bars show the RSCU values of synonymous codons for each amino acid (single-letter code on the x-axis; "*" indicates stop codons). Each bar segment is labeled with the codon and its RSCU value, and synonymous codons are arranged from higher (bottom) to lower (top) RSCU values

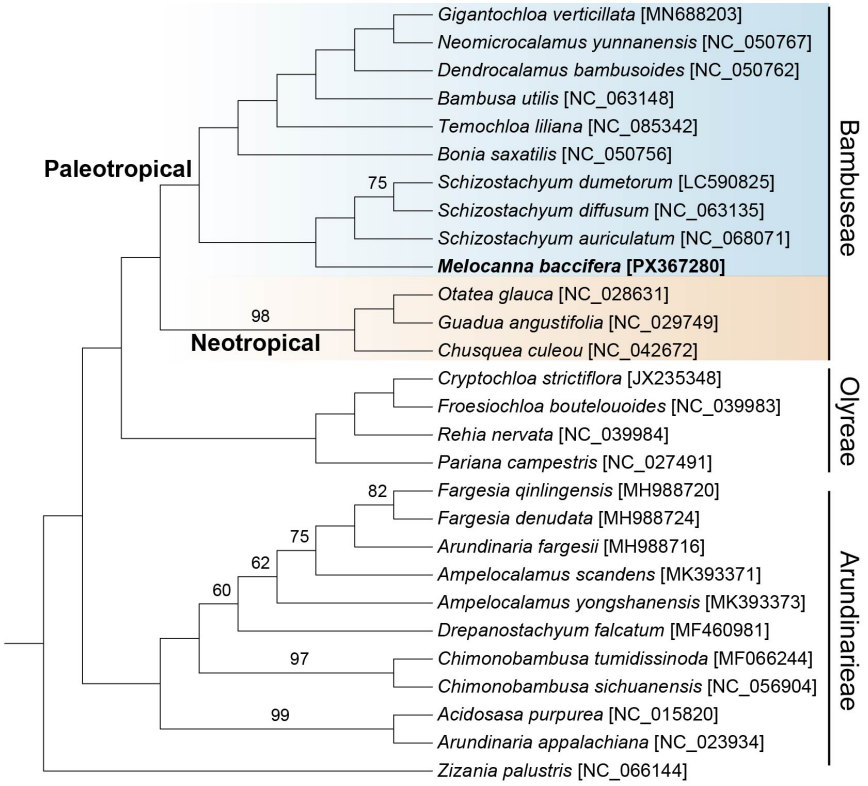

Figure 7. Maximum likelihood phylogeny of Bambusoideae inferred from 73 chloroplast protein-coding sequences. The tree is shown as a cladogram, due to the close relationships within the subfamily. Tip labels include species names and GenBank accession numbers. Node numbers indicate bootstrap support; maximal values are omitted for clarity. Tribe names are displayed on the right side of the tree

Neotropical lineage included *Otatea*, *Guadua*, and *Chusquea*. The three *Schizostachyum* species and *M. baccifera* formed a well-supported clade, indicating that *M. baccifera* was sister to the *Schizostachyum* clade.

4. Discussion

4.1. Chloroplast Genome Features in The Bambuseae Tribe

M. baccifera undergoes a characteristic cycle of gregarious flowering, fruiting, and post-reproductive clump mortality, a phenomenon that may trigger rodent outbreaks, increase fuel loads after mass die-off, and exacerbate the effects of habitat disturbance and land-use change (Koshy *et al*. 2022). In addition, population decline in natural habitats, together with losses of fruits and seeds to animals and insects, has been reported, indicating that local populations may be vulnerable to genetic erosion and seed-source bias in the absence of an appropriate genetic monitoring framework (Nilkanta *et al*. 2017; Fava and Colombo 2017). Therefore, the development of genomic resources for *M. baccifera* should be regarded as urgent of establish a local reference dataset for species identification, provenance tracing, genetic diversity assessment, and the selection of suitable planting material and restoration sources following gregarious flowering events. The complete cp genome of *M. baccifera*, characterized in this study, exhibited the typical quadripartite structure of angiosperm plastomes. However, comparison with related Bambuseae revealed lineage-specific features that provided insight into both plastome evolution and the phylogenetic position of this tribe. Comparative plastome data suggested that the sampled Paleotropical woody bamboos were more structurally conserved than the sampled Neotropical taxa in overall cp genome structure. All Paleotropical species shared the same GC content (38.9%) and showed only minor variation in total plastome size and regional lengths, indicating a high level of structural stability within this lineage. By contrast, the Neotropical taxa exhibited slightly lower GC content and greater variation in plastome size, which was mainly associated with reductions in IR length in *O. glauca* and *G. angustifolia*, and with LSC contraction in *C. culeou*. Within this framework, *M. baccifera* closely matched the Paleotropical pattern in genome size, GC content, and regional organization, supporting its placement within the structurally conserved Paleotropical woody bamboo lineage rather than the more variable Neotropical group (Wysocki *et al*. 2015; Wang *et al*. 2020).

Our MAUVE alignment indicated that Bambuseae plastomes were structurally stable, as the same local collinear blocks were present in the same order across all eight genomes (Figure 2), with no evidence of large inversions or translocations. This high level of synteny was consistent with earlier whole-plastome comparisons in woody bamboos, in which complete cp genomes generally exhibited conserved gene content and gene order, with phylogenetic signal arising mainly from sequence variation rather than genome rearrangements (Zhang *et al*. 2011). Recent studies on Bambusoideae also reported strong collinearity and broadly conserved plastome architecture across closely related bamboo lineages, supporting the idea that genome structure was constrained within the group (Wang *et al*. 2024). In our study, the four IR junctions (JLB, JSB, JSA, and JLA) were also largely conserved, consistent with patterns reported for multiple bamboo genera, including *Bambusa* and *Phyllostachys*, in which boundary-associated genes such as *rpl22*, *rps19*, *ndhF*, *ndhH*, and *psbA* were located near the junctions (Liu *et al*. 2024). In contrast, frequent IR expansions and contractions were reported in Olyreae, leading to reductions in the copy numbers of *rps19* and *trnH-GUG* in *Froesiochloa*. In contrast, our Bambuseae sampling showed only subtle shifts in boundaries (Wang *et al*. 2018). At the broader family scale, Poaceae plastomes were known to contain ancient, lineage-defining structural events, including the classic 28-kb and 6-kb inversions and several gene and intron losses. Therefore, the absence of large rearrangements among our Bambuseae taxa suggested that most major structural changes had occurred deeper in grass evolution rather than within bamboo lineages (Doyle *et al*. 1992). Overall, these results indicated that Bambuseae plastomes remained highly conserved in structure, with only minor IR-boundary shifts and lineage-specific IR length variation.

In the *M. baccifera* cp genome, 44 SSRs were detected, with a strong predominance of A/T mononucleotide motifs and a distribution mainly concentrated in the LSC region, consistent with the widely recognized "grass-type" plastome pattern (Liu *et al*. 2022; Pei *et al*. 2022). Similar A/T-biased cpSSRs and LSC-skewed distributions were reported in other bamboos, such as *Chimonobambusa hirtinoda* and *Dendrocalamus farinosus*, as well as in broader Poaceae comparisons involving *Secale* and *Pennisetum* plastomes, suggesting that this feature was conserved across Bambusoideae and Poaceae (Skuza & Jastrzębski 2025). Although only 10 long repeats were detected in *M. baccifera*, most

were forward repeats and were mainly distributed in the LSC region. Their type and regional distribution were consistent with observations from many other bamboo plastomes, whereas differences in repeat number among studies likely reflected variation in repeat-detection thresholds and analytical pipelines (Zhang *et al*. 2011; Huang *et al*. 2025). The concentration of repeats in the LSC region may also help explain why diverging hotspots in bamboo and grass plastomes were frequently associated with repeat-rich intergenic regions, even though the overall plastome structure remained highly conserved. Codon usage in *M. baccifera* (19,879 codons) showed that leucine was the most abundant amino acid and that preferred synonymous codons largely ended in A/T, mirroring patterns reported for other Bambuseae and Poaceae plastomes (Zhang *et al*. 2012). At the family level, Poaceae cp genomes also showed an overrepresentation of NNA/NNT codons, consistent with mutation pressure related to base composition and natural selection jointly shaping codon usage bias (Zhang *et al*. 2012). Overall, the repeat landscape and codon usage pattern of *M. baccifera* indicated a typical A/T-rich grass plastome, while also providing a useful set of cpSSR and repeat loci that could be developed as molecular markers for genetic diversity and lineage differentiation in *Melocanna* and closely related Bambuseae taxa.

Our sliding-window analysis showed that cp sequence divergence among Bambuseae species was generally low, supporting a highly conserved plastome. This pattern has also been widely reported in bamboos and other Poaceae lineages (Zhang *et al*. 2011). The strongest signal of variation occurred in the LSC, with the highest peak at the *trnG-trnT* intergenic spacer, indicating that informative polymorphisms were primarily concentrated in this region (Wang *et al*. 2024). Notably, *trnG-trnT* has also been identified as a hypervariable locus in other bamboo plastome comparisons (*Gelidocalamus* and *Stipa* genera), suggesting that it represented a robust candidate marker for fine-scale discrimination within Bambuseae when complete plastome sequences were unavailable (Wang *et al*. 2024). Overall, our results supported the use of *trnG-trnT* as a practical barcode and phylogeographic marker that could complement complete-plastome approaches in Bambuseae.

4.2. Phylogenetic Placement of *Melocanna baccifera* Within The Family Bambusoideae

The ML tree inferred from 73 cp protein-coding regions recovered the three tribes of Bambusoideae (Bambuseae, Olyreae, and Arundinarieae) as well-supported monophyletic groups, consistent with previous plastome- and multigene studies (Kelchner *et al*. 2013; Ma *et al*. 2014; Wysocki *et al*. 2015). Within Bambuseae, the topology clearly separated Paleotropical and Neotropical woody bamboos, in agreement with earlier phylogenetic analyses based on plastid and nuclear markers (Sungkaew *et al*. 2009; Zhou *et al*. 2017; Wang *et al*. 2020). *M. baccifera* was resolved with high support (bootstrap = 98) as sister to a clade of *Schizostachyum* species within the Paleotropical bamboo lineage. This placement is consistent with recent plastid phylogenomic analyses of Melocanninae, which showed that *Melocanna*, *Schizostachyum*, and related genera form a closely allied group within Paleotropical woody bamboos (Zhou *et al*. 2022; Liu *et al*. 2024).

Earlier studies based on a limited number of plastid and nuclear loci often produced unstable or conflicting placements for Melocanninae, likely due to insufficient phylogenetic signal as well as the effects of hybridization and incomplete lineage sorting (Sungkaew *et al*. 2009; Zhang *et al*. 2012; Goh *et al*. 2013; Chalopin *et al*. 2021; Cai *et al*. 2023). In contrast, the plastome-scale dataset used here provided a stable and well-supported phylogenetic position for *M. baccifera* within Paleotropical Bambuseae. This relationship is further supported by both plastome structural comparisons and recent Melocanninae-focused phylogenomic analyses, which consistently indicate a close affinity between *M. baccifera* and *Schizostachyum* (Zhou *et al*. 2022).

4.3. Taxonomic and Evolutionary Implications and Future Directions

The cp characteristics and phylogenetic position of *M. baccifera* indicated that it was a structurally conserved but morphologically specialized member of the Paleotropical woody bamboo lineage. The cp genome did not show unusual rearrangements, gene losses, or conspicuous IR asymmetries that would suggest a deeply divergent plastome lineage. Instead, it closely matched the structural profile of *Schizostachyum* and other Melocanninae in terms of genome size, GC content, and IR-SC boundary structure (Zhou *et al*. 2022; Liu *et al*. 2024). Thus, the distinctive fleshy fruit and monocarpic life history of *M. baccifera* do not appear to be associated with obvious plastome-specific changes in our data and are primarily related to nuclear genomic evolution. This pattern fitted the broader view that major morphological transitions in Paleotropical woody bamboos often occurred against a background of plastome stability (Wysocki *et al*. 2015; Liu *et al*. 2024). From a taxonomic perspective, our

results supported the current placement of *Melocanna* within Melocanninae and reinforced its close affinity with *Schizostachyum*. The strong plastome-based phylogeny support for a *Melocanna-Schizostachyum* clade, together with their shared plastome architecture, supports a close relationship between the two genera in future taxonomic treatments. At the same time, the pronounced differences in fruit morphology and culm characteristics justified maintaining them as distinct genera, in line with phylogenomic frameworks that recognize morphologically coherent genera within Melocanninae (Zhou *et al*. 2017, 2022; Liu *et al*. 2024).

The complete cp genome of *M. baccifera* provided a genomic reference for developing molecular markers and addressing evolutionary questions at multiple scales. Hypervariable noncoding regions, such as *trnH-psbA*, *rpl32-trnL*, and other intergenic spacers, have proven useful in other angiosperms and bamboos (Ma *et al*. 2014; Liu *et al*. 2020) and could be evaluated in *Melocanna* for their potential applications in population genetics, phylogeography, and conservation assessments. Combining such plastid markers with nuclear loci will be crucial for testing hypotheses of reticulate evolution and incomplete lineage sorting that have emerged from studies of Paleotropical woody bamboos (Chalopin *et al*. 2021; Cai *et al*. 2023).

In conclusion, this study reported the complete cp genome of *M. baccifera* and refined its phylogenetic placement of within Bambusoideae. The genomic resources generated here provided a useful foundation for future phylogenomic and evolutionary studies. Expanded sampling within Melocanninae and other poorly represented Paleotropical bamboo lineages will further improve our understanding of bamboo diversification and evolutionary history. Moreover, the *M. baccifera* cp genome can now be used to develop molecular markers for population genetics and breeding programs, thereby helping to address critical gaps in the effective stewardship of this valuable species.

Acknowledgements

Minh Trong Quang was funded by the Master's and PhD Scholarship Program of Vingroup Innovation Foundation, code VINIF.2021.ThS.69 and VINIF.2022.ThS.054.

Conflicts of Interest

The authors declare no conflicts of interest.

Data Available

The genome sequence data supporting the findings of this study are openly available in GenBank under accession number PX367280.

References

Amiryousefi, A., Hyvönen, J., Poczai, P., 2018. IRscope: an online program to visualize the junction sites of chloroplast genomes. *Bioinformatics*. 34, 3030–3031. https://doi.org/10.1093/bioinformatics/bty220

Bolger, A. M., Lohse, M., Usadel, B., 2014. Trimmomatic: a flexible trimmer for Illumina sequence data. *Bioinformatics*, 30, 2114–2120. https://doi.org/10.1093/bioinformatics/btu170

Cai, Z.Y., Niu, Z.Y., Zhang, Y.Y., Tong, Y.H., Vu, T.C., Goh, W.L., Sungkaew, S., Teerawatananon, A., Xia, N.H., 2023. Phylogenomic analyses reveal reticulate evolution between *Neomicrocalamus* and *Temochloa* (Poaceae: Bambusoideae). *Front Plant Sci*. 14, 1274337. https://doi.org/10.3389/fpls.2023.1274337

Capella-Gutiérrez, S., Silla-Martínez, J.M., Gabaldón, T., 2009. trimAl: a tool for automated alignment trimming in large-scale phylogenetic analyses. *Bioinformatics*, 25, 1972-1973. https://doi.org/10.1093/bioinformatics/btp348

Chalopin, D., Clark, L.G., Wysocki, W.P., Park, M., Duvall, M.R., Bennetzen, J.L., 2021. Integrated genomic analyses from low-depth sequencing help resolve phylogenetic incongruence in the Bamboos (Poaceae: Bambusoideae). *Front Plant Sci*. 12, 725728. https://doi.org/10.3389/fpls.2021.725728

Chan, P.P., Lin, B.Y., Mak, A.J., Lowe, T.M., 2021. tRNAscan-SE 2.0: improved detection and functional classification of transfer RNA genes. *Nucleic Acids Res*. 49, 9077-9096. https://doi.org/10.1093/nar/gkab688

Darling, A.C., Mau, B., Blattner, F.R., Perna, N.T., 2004. Mauve: Multiple alignment of conserved genomic sequence with rearrangements. *Genome Res*. 14, 1394-1403. https://doi.org/10.1101/gr.2289704

Dierckxsens, N., Patrick, M., Guillaume, S, 2017. NOVOPlasty: de novo assembly of organelle genomes from whole genome data. *Nucleic Acids Res*. 45, e18. https://doi.org/10.1093/nar/gkw955

Doyle, J.J., Davis, J.I., Soreng, R.J., Garvin, D., Anderson, M.J., 1992. Chloroplast DNA inversions and the origin of the grass family (Poaceae). *Proc Natl Acad Sci U S A*. 89, 7722-7726. https://doi.org/10.1073/pnas.89.16.7722

Fava, F., Colombo, R., 2017. Remote sensing-based assessment of the 2005–2011 bamboo reproductive event in the Arakan mountain range and its relation with wildfires. *Remote Sens*. 9, 85. https://doi.org/10.3390/rs9010085

Fisher, A.E., Clark, L.G., Kelchner, S.A., 2014. Molecular phylogeny estimation of the Bamboo genus *Chusquea* (Poaceae: Bambusoideae: Bambuseae) and description of two new subgenera. *Syst Bot*. 39, 829-844. https://doi.org/10.1600/036364414X681554

Goh, W.L., Chandran, S., Franklin, D.C., Isagi, Y., Koshy, K.C., Sungkaew, S., Yang, H.Q., Xia, N.H., Wong, K.M., 2013. Multi-gene region phylogenetic analyses suggest reticulate evolution and a clade of Australian origin among paleotropical woody bamboos (Poaceae: Bambusoideae: Bambuseae). *Plant Systematics and Evolution*. 299, 239–257. https://doi.org/10.1007/s00606-012-0718-1

Greiner, S., Lehwark, P., Bock, R., 2019. OrganellarGenomeDRAW (OGDRAW) version 1.3.1: expanded toolkit for the graphical visualization of organellar genomes. *Nucleic Acids Res*. 47, W59-W64. https://doi.org/10.1093/nar/gkz238

Huang, S., Yu, G., Wang, Y., Gao, H., Hui, C., Vasupalli, N., Lin, X., 2025. Chloroplast genome analysis of *Dendrocalamus* × *mutatus* and its implications for bamboo classification. *BMC Plant Biol*. 25, 1177. https://doi.org/10.1186/s12870-025-07199-x

Huynh, T.T., Quang, M.T., Nguyen, H.D., 2024. The complete chloroplast genome of *Syzygium syzygioides* (Myrtaceae: Myrtales) and phylogenetic analysis. *Biomed Biotechnol Res J*. 8, 409-414. https://doi.org/10.4103/bbrj.bbrj_233_24

Jansen, R.K., Cai, Z., Raubeson, L. A., Daniell, H., Depamphilis, C.W., Leebens-Mack, J., Müller, K. F., Guisinger-Bellian, M., Haberle, R.C., Hansen, A.K., Chumley, T.W., Lee, S.B., Peery, R., McNeal, J.R., Kuehl, J.V., Boore, J.L., 2007. Analysis of 81 genes from 64 plastid genomes resolves relationships in angiosperms and identifies genome-scale evolutionary patterns. *Proc Natl Acad Sci U S A*. 104, 19369-19374. https://doi.org/10.1073/pnas.0709121104

Kalyaanamoorthy, S., Minh, B.Q., Wong, T.K.F., von Haeseler, A., Jermiin, L.S., 2017. ModelFinder: fast model selection for accurate phylogenetic estimates. *Nat Methods*. 14, 587-589. https://doi.org/10.1038/nmeth.4285

Katoh, K., Standley, D.M., 2016. A simple method to control over-alignment in the MAFFT multiple sequence alignment program. *Bioinformatics*, 32, 1933-1942. https://doi.org/10.1093/bioinformatics/btw108

Kelchner, S.A., Clark, L., Cortés, G., Oliveira, R.P., Dransfield, S., Filgueiras, T., Fisher, A.E., Guala, G.F., Hodkinson, T., Judziewicz, E., Kumar, M., Li, D.Z., Londoño, X., Teresa Mejia, M., Santos-Gonçalves, A.P., Stapleton, C., Sungkaew, S., Triplett, J., Widjaja, E., Wong, K.M., Xia, N.H., 2013. Higher level phylogenetic relationships within the bamboos (Poaceae: Bambusoideae) based on five plastid markers. *Mol Phylogenet Evol*. 67, 404–413. https://doi.org/10.1016/j.ympev.2013.02.005

Koshy, K.C., Gopakumar, B., Sebastian, A., S, A.N., Johnson, A.J., Govindan, B., Baby, S., 2022. Flower-fruit dynamics, visitor-predator patterns and chemical preferences in the tropical bamboo, *Melocanna baccifera*. *Plos one.* 17, e0277341. https://doi.org/10.1371/journal.pone.0277341

Kurtz, S., 2001. REPuter: the manifold applications of repeat analysis on a genomic scale. *Nucleic Acids Res*. 29, 4633-4642. https://doi.org/10.1093/nar/29.22.4633

Le, S., Nguyen, T.H., Quang, M.T., 2025. The complete chloroplast genome sequence of *Cinnamomum balansae* and its phylogenetic implications. *Korean J Plant Taxon*. 55, 70-75. https://doi.org/10.11110/kjpt.2025.55.2.70.

Letunic, I., Bork, P., 2024. Interactive Tree of Life (iTOL) v6: recent updates to the phylogenetic tree display and annotation tool. *Nucleic Acids Res*. 52, W78-W82. https://doi.org/10.1093/nar/gkae268

Liu, Q., Li, X., Li, M., Xu, W., Schwarzacher, T., Heslop-Harrison, J.S., 2020. Comparative chloroplast genome analyses of Avena: Insights into evolutionary dynamics and phylogeny. *BMC Plant Biol*. 20, 1-20. https://doi.org/10.1186/s12870-020-02621-y

Liu, Y., Zhu, X., Wu, M., Xu, X., Dai, Z., Gou, G., 2022. The complete chloroplast genome of critically endangered *Chimonobambusa hirtinoda* (Poaceae: Chimonobambusa) and phylogenetic analysis. *Sci Rep*. 12, 9649. https://doi.org/10.1038/s41598-022-13204-2

Liu, J.X., Guo, C., Ma, P.F., Zhou, M.Y., Luo, Y.H., Zhu, G.F., Xu, Z.C., Milne, R.I., Vorontsova, M.S., Li, D.Z., 2024. The origin and morphological character evolution of the paleotropical woody bamboos. *J Integr Plant Biol*. 66, 2242. https://doi.org/10.1111/jipb.13751

Liu, Y., Xu, H., Liu, X., Li, X., Chen, G., Wei, X., Wang, Y., Jin, C., Wang, J., Xia, H., 2024. Genome survey and complete chloroplast genome structure of a bamboo species (*Bambusa grandis*) provide a useful basis in genomic research. *ScienceAsia*. 50, 1. https://doi.org/10.2306/scienceasia1513-1874.2024.083

Ma, P.F., Zhang, Y.X., Zeng, C.X., Guo, Z.H., Li, D.Z., 2014. Chloroplast phylogenomic analyses resolve deep-level relationships of an intractable bamboo tribe Arundinarieae (Poaceae). *Syst Biol*. 63, 933-950. https://doi.org/10.1093/sysbio/syu054

Minh, B.Q., Schmidt, H.A., Chernomor, O., Schrempf, D., Woodhams, M.D., Von Haeseler, A., Lanfear, R., Teeling, E., 2020. IQ-TREE 2: New Models and Efficient Methods for Phylogenetic Inference in the Genomic Era. *Mol Biol Evol*. 37, 1530-1534. https://doi.org/10.1093/molbev/msaa015

Nilkanta, H., Amom, T., Tikendra, L., Rahaman, H., Nongdam, P., 2017. ISSR marker based population genetic study of *Melocanna baccifera* (Roxb.) Kurz: a commercially important bamboo of Manipur, North-East India. *Scientifica*. 3757238. https://doi.org/10.1155/2017/3757238

Parks, M., Cronn, R., Liston, A., 2009. Increasing phylogenetic resolution at low taxonomic levels using massively parallel sequencing of chloroplast genomes. *BMC Biol*. 7, 1-17. https://doi.org/10.1186/1741-7007-7-84

Pei, J., Wang, Y., Zhuo, J., Gao, H., Vasupalli, N., Hou, D., Lin, X., 2022. Complete chloroplast genome features of *Dendrocalamus farinosus* and its comparison and evolutionary analysis with other Bambusoideae species. *Genes*. 13, 1519. https://doi.org/10.3390/genes13091519

Porebski, S., Bailey, L.G., Baum, B.R., 1997. Modification of a CTAB DNA extraction protocol for plants containing high polysaccharide and polyphenol components. *Plant Mol Biol Rep*. 15, 8-15. https://doi.org/10.1007/BF02772108

Quang, M.T., Huynh, T.T., 2024. Complete chloroplast genome of *Syzygium glomeratum* (Myrtaceae) and phylogenetic analysis. *Korean J Plant Taxon*. 54, 316–322. https://doi.org/10.11110/kjpt.2024.54.4.316

Rathour, R., Kumar, H., Prasad, K., Anerao, P., Kumar, M., Kapley, A., Pandey, A., Kumar Awasthi, M., Singh, L., 2022. Multifunctional applications of bamboo crop beyond environmental management: an Indian prospective. *Bioengineered*. 13, 8893-8914. https://doi.org/10.1080/21655979.2022.2056689

Rozas, J., Ferrer-Mata, A., Sánchez-DelBarrio, J.C., Guirao-Rico, S., Librado, P., Ramos-Onsins, S.E., Sánchez-Gracia, A., 2017. DNASP 6: DNA sequence polymorphism analysis of large data sets. *Mol Biol Evol*. 34, 3299-3302. https://doi.org/10.1093/molbev/msx248

Shaw, J., Lickey, E.B., Schilling, E.E., Small, R.L., 2007. Comparison of whole chloroplast genome sequences to choose noncoding regions for phylogenetic studies in angiosperms: The Tortoise and the hare III. *Am J Bot*. 94, 275–288. https://doi.org/10.3732/AJB.94.3.275

Skuza, L., Jastrzębski, J.P., 2025. The complete chloroplast genome of Secale strictum ssp. strictum provides insights into Triticeae evolution and breeding. *Sci Rep*. 15, 42882. https://doi.org/10.1038/s41598-025-27062-1

Sungkaew, S., Stapleton, C.M.A., Salamin, N., Hodkinson, T.R., 2009. Non-monophyly of the woody bamboos (Bambuseae; Poaceae): A multi-gene region phylogenetic analysis of Bambusoideae s.s. *J Plant Res*. 122, 95–108. https://doi.org/10.1007/S10265-008-0192-6

Sutherland, D.M., Clayton, W.D., Renvoize, S.A., 1987. Genera graminum. Grasses of the world. *Brittonia*. 39, 508-508. https://doi.org/10.2307/2807332

Telonis, A.G., Margarity, M., 2015. Phobos: A novel software for recording rodents' behavior during the thigmotaxis and the elevated plus-maze test. *Neurosci Lett*. 599, 81-85. https://doi.org/10.1016/j.neulet.2015.05.045

Tillich, M., Lehwark, P., Pellizzer, T., Ulbricht-Jones, E.S., Fischer, A., Bock, R., Greiner, S., 2017. GeSeq – versatile and accurate annotation of organelle genomes. *Nucleic Acids Res*. 45, W6–W11. https://doi.org/10.1093/nar/gkx391

Triplett, J.K., Clark, L.G., 2010. Phylogeny of the temperate Bamboos (Poaceae: Bambusoideae: Bambuseae) with an emphasis on arundinaria and allies. *Syst Bot*. 35, 102–120. https://doi.org/10.1600/036364410790862678

Vorontsova, M.S., Clark, L.G., Dransfield, J., Govaerts, R., Baker, W.J., 2017. World checklist of bamboos and rattans. Royal Botanic Gardens, Kew.

Wang, W., Chen, S., Zhang, X., 2018. Whole-Genome comparison reveals divergent IR borders and mutation hotspots in chloroplast genomes of herbaceous bamboos (Bambusoideae: Olyreae). *Molecules*. 23, 1537. https://doi.org/10.3390/molecules23071537

Wang, W., Chen, S., Guo, W., Li, Y., Zhang, X., 2020. Tropical plants evolve faster than their temperate relatives: a case from the bamboos (Poaceae: Bambusoideae) based on chloroplast genome data. *Biotechnol Biotechnol Equip*, 34, 482-493. https://doi.org/10.1080/13102818.2020.1773312

Wang, C., Li, Y., Yang, G., Zhang, W., Guo, C., 2024. Comparative analysis of chloroplast genomes and phylogenetic relationships in the endemic Chinese bamboo *Gelidocalamus* (Bambusoideae). *Front Plant Sci*. 15, 1470311. https://doi.org/10.3389/fpls.2024.1470311

Wang, W., Wu, Q., Wang, N., Ye, S., Wang, Y., Zhang, J., Lin, C., Zhu, Q., 2025. Advances in bamboo genomics: Growth and development, stress tolerance, and genetic engineering. *J Integr Plant Biol*. 67, 1725-1755. https://doi.org/10.1111/jipb.13909

Wicke, S., Schneeweiss, G.M., dePamphilis, C.W., Müller, K.F., Quandt, D., 2011. The evolution of the plastid chromosome in land plants: Gene content, gene order, gene function. *Plant Mol Biol*. 76, 273-297. https://doi.org/10.1007/s11103-011-9762-4

Wysocki, W.P., Clark, L.G., Attigala, L., Ruiz-Sanchez, E., Duvall, M.R., 2015. Evolution of the bamboos (Bambusoideae; Poaceae): A full plastome phylogenomic analysis Genome evolution and evolutionary systems biology. *BMC Evol Biol*. 15, 1-12. https://doi.org/10.1186/s12862-015-0321-5

Zhang, Y.J., Ma, P.F., Li, D.Z., 2011. High-throughput sequencing of six bamboo chloroplast genomes: Phylogenetic implications for temperate woody bamboos (Poaceae: Bambusoideae). *PLoS One*. 6, e20596. https://doi.org/10.1371/journal.pone.0020596

Zhang, Y., Nie, X., Jia, X., Zhao, C., Biradar, S.S., Wang, L., Du, X., Weining, S., 2012. Analysis of codon usage patterns of the chloroplast genomes in the Poaceae family. *Aust J Bot*. 60, 461–470. https://doi.org/10.1071/bt12073

Zhang, Y.X., Zeng, C.X., Li, D.Z., 2012. Complex evolution in Arundinarieae (Poaceae: Bambusoideae): Incongruence between plastid and nuclear GBSSI gene phylogenies. *Mol Phylogenet Evol*. 63, 777-797. https://doi.org/10.1016/j.ympev.2012.02.023

Zhou, M.Y., Zhang, Y.X., Haevermans, H., Li, D.Z., 2017. Towards a complete generic-level plastid phylogeny of the paleotropical woody bamboos (Poaceae: Bambusoideae). *Taxon*. 66, 539-553. https://doi.org/10.12705/663.2

Zhou, M.Y., Liu, J.X., Ma, P.F., Yang, J.B., Li, D.Z., 2022. Plastid phylogenomics shed light on intergeneric relationships and spatiotemporal evolutionary history of Melocanninae (Poaceae: Bambusoideae). *J Syst Evol*. 60, 640-652. https://doi.org/10.1111/jse.12843